

Flux Trapping and Field Magnet Stability of Bulk Superconductors

YF Zhang¹, W Zhou¹, Y Xu¹, B Li², D Zhou², K Tsuzuki^{2,3}, M Watasaki², M Miki² and M Izumi²

¹Shanghai University of Electric Power, New Pudong, Shanghai 201300, China

²Tokyo University of Marine Science and Technology, Tokyo 135-8533, Japan

³Toba National College of Maritime Technology, Mie 517-8501, Japan

Abstract. The stability and durability of trapped flux is a focus in investigations of melt-growth (RE)Ba₂Cu₃O_{7-δ} (RE=rare earth, e.g., Y, Gd, Sm) bulk high-temperature superconductors. In magnetic flux engineering applications, two important issues affect the expected performance of bulk superconductors: flux trapping and flux stability or durability. The introduction of effective pinning with homogeneous spatial distribution is inevitable. The materials process and durability studies have been pursued in the last decade with either a stationary or a momentary applied external field. In machine applications, the magnetic flux stability is influenced by external perturbations. We topically summarize our progress and current status in relation to past and ongoing work.

1. Introduction

Melt-growth (RE)Ba₂Cu₃O_{7-δ} (RE=rare earth Y, Gd, Sm, etc.) bulk high-temperature superconductors have attracted interest for their potential applications, and trapped flux densities of 17 T at 29 K [1] and 3 T at 77 K [2] have been shown. The enhanced critical current density (J_c) based on flux pinning is a key issue for industrial applications [3]. An improvement in J_c under a magnetic field has been reported by introducing the possible interface between the non-superconducting and superconducting phases. A variety of strategies and techniques have been developed to improve the flux pinning and the homogeneity of materials. During the melt-growth process, intrinsic pinning could be introduced through the effects of stacking faults, low angle grain boundaries, twin boundaries, precipitates, impurity phases, secondary phases, point defects, oxygen vacancies, growth dislocation, structural inhomogeneity, and other objects with different dimensionality. In addition, so-called chemical doping with ionic substitution has been widely investigated, in which Fe, Co, and/or Ga is preferentially substituted to at Cu-O chain sites [4]. On the other hand, for example, Ni or Ti may occupy the Cu-O plane and may affect the superconductivity of the mother phase bulks by way of local lattice distortion [4].

Another strategy to achieve high flux pinning is the addition of fine particles such as nanometre-sized second phase RE₂BaCuO₅ (RE211), RE₂Ba₄CuMO_y (RE2411, Mo, Zr), or other metal oxides. This meets the requirements for a short coherence length close to about 2-4 nm below 77 K [5]. The *in situ* formation of nanosized BaZrO₃ or others have been reported. The J_c of the portion taken below the seeding site in the melt-growth bulks is considerably high, and the trapped flux density exhibits a peak value larger than that of conventional permanent magnets. A couple of viewpoints are considered in industrial applications: the maximization of the trapped flux intensity by enhanced J_c , or the



optimization of the trapped flux and its stability and durability under a variety of external field and temperature perturbations. In this paper, we summarize and review several key issues and describe our activities.

2. Critical current density

Xu *et al.* [6] extensively studied c-axis-oriented, single-domain $\text{GdBa}_2\text{Cu}_3\text{O}_{7-d}$ (Gd123) melt-textured bulk superconductors. First, they clarified the solubility of the solid solution with $\text{Gd}_{1+x}\text{Ba}_{2-x}\text{Cu}_3\text{O}_{7-\delta}$ ($x < 0.1$), but found a remarkable inhomogeneous distribution and ripening of Gd211. With this limitation in the refinement of the Gd211 addition due to the pushing/trapping effect and ripening, nano-Gd211 inclusion was difficult to induce. Thus, another kind of material was synthesized, the Gd2411 single phase. The J_c value was dependent on the positions because there was an inhomogeneous distribution of these second phases. However, the highest J_c was $84,500 \text{ A/cm}^2$ at a liquid nitrogen temperature under the self-field. Gd2411 has been observed to exist in an RE123 matrix with a size of several nanometres and it improves J_c . Nanosized particles were doped into Gd123 bulks, which displayed enhanced superconducting properties with the optimum additional amount. SEM results showed an inhomogeneous distribution of Gd211 appearing around the seeding site in the bulk, even when the doping amount was quite low. ZrO_2 or SnO_2 nanosized particles reacted with the Gd123 matrix before the melt process to form BaZrO_3 or BaSnO_3 particles *in situ*, with an average diameter of approximately 50 nm. These played a role in the effective flux pinning. BaZrO_3 nanosized particles were embedded in the Gd211 particles and contributed to the size reduction of the latter. Enhanced superconductivity in Gd123 has been achieved for the J_c value in an air process of $100,000 \text{ A/cm}^2$ at 77 K and a self-field [7]. The trapped field was up to 0.7 T for bulk $\phi = 24 \text{ mm}$. Using atomic force microscopy (AFM), nanostripes with a wavelength of 15 nm were observed in the ZnO-doped Gd123 sample. Nanosized particles in the grown Gd123 single domain, together with micro-defects induced by particle doping, can account for the enhanced superconducting properties.

The magnetic particle of Fe-B alloys (e.g., $\text{Fe}_{0.69}\text{B}_{0.12}\text{Si}_{0.14}\text{Nb}_{0.03}\text{Cr}_{0.01}\text{Cu}_{0.01}$) was added by Xu [8] for the first time in Gd123 bulk superconductors. Suitable amounts of magnetic particle inclusions resulted in the enhancement of J_c in the bulk. Xu *et al.* [9] found that the maximum trapped field of the sample with 0.4 mol% Fe-B alloy particles reached 0.16 T, which was 31% higher than that without Fe-B additives. Tsuzuki *et al.* [10] studied the effect of addition for Fe-Si, Fe-Si-Al, and Fe-Si-B-Cr-C alloys in the Gd123+Gd211 matrix. The trapped flux of the Fe-B doped and Fe-Si doped samples considerably exceeded those of the undoped samples. A value of $B = 0.16 \text{ T}$ was obtained for the local maximum in the centre of the top surface in the Fe-Si and Fe-Si-B-Nb-Cr-Cu doped samples. For the result of Fe-B in the 0.4 mol% doped samples, the value of the trapped magnetic flux was $8.80 \mu\text{Wb}$, which is 14% higher than that for the undoped samples. The Fe-Si addition marked $8.17 \mu\text{Wb}$. The bulk Gd123 with doping by several magnetic particles (MP) provided an intensified trapped magnetic flux compared with those without the addition. The reason is possibly that the Fe-containing particles contributed to a reduction in the interfacial energy of Gd211 and increased the nucleation sites with fine dimensions, thus preventing the Gd211 coarsening.

Li *et al.* [11] studied the pinning effect of Gd123 bulk, with different doping amounts of BaTiO_3 up to 0.4 mol%. The J_c showed the existence of two optimized doping levels. One was at 0.1 mol% addition, in which the J_c was enhanced around the zero field and the middle field of 1.5 T. The other was 0.3 mol% with a J_c value close to that for the 0.1 mol% doped bulk around the zero field; however, it exhibited a lower peak. The highest J_c of $3.8 \times 10^4 \text{ A/cm}^2$ was achieved in 0.1 BTO [11]. A 0.3 mol% BTO addition mainly contributed to the enhancing flux pinning under a low field. Using a similar method, Li *et al.* [12] studied Gd123 with a TiO_2 addition. The TiO_2 doping resulted in improved T_c and enhanced δl pinning. The BaTiO_3 doped sample exhibited a maximum around the zero field (Fig 1). From this it was concluded that the nanometre-sized TiO_2 dilute addition has the ability to enhance flux pinning under a low field.

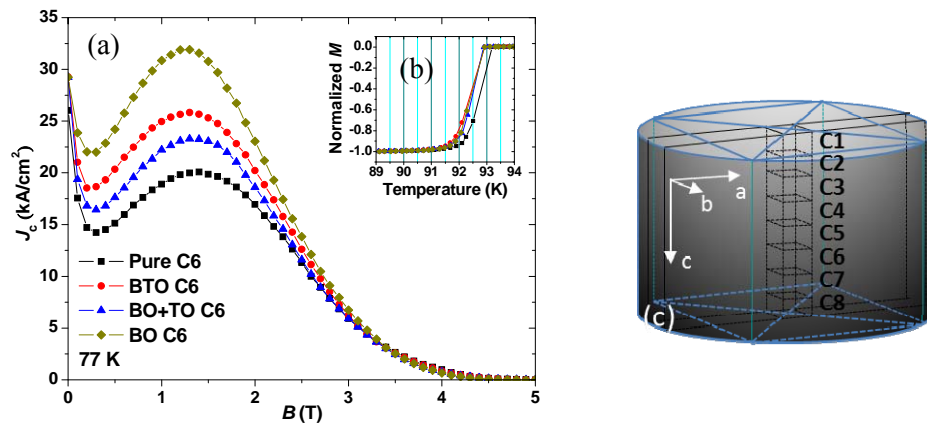


Fig. 1 Critical current density as a function of (a) magnetic field and (b) the critical transition temperature for Gd123 (pure), Gd123 with BaTiO₃ (BTO), BaO₂+TiO₂ (BO+TO), and BaO₂ (BO) additions. The samples were taken from C6 as indicated in (c).

Based on the nature of liquid dispersion and the anisotropic growth of the matrix, Li *et al.* [12] addressed the recrystallization of fine inclusions related to the employment of BaTiO₃. The recrystallization may overcome the disadvantage of the pushing effect and encourages the *in situ* formation of fine particles other than the starting powder. These results demonstrated that the flux pinning performance was greatly improved, and the self-field J_c value reached 52.5 kA/cm². The onset transition temperature was improved as a result of the lower starting growth temperature. These results showed that the BTO doping-related precipitations are independent of the matrix, and the positive effect of recrystallization of the finer inclusions is reasonably verified by growing the bulk at the lower initial growth temperature. The contribution of Gd211 on the enhancement of flux pinning is finite because the main Gd211 particles are still in the micrometre range. Therefore, the significantly increased pinning performance along the c -axis in a low field was additionally attributed to the recrystallization of the finer BTO doping-related precipitation, due to the anisotropic crystal growth. As shown in Fig. 1, the aligned peaks should come from the anisotropic crystal growth since it unavoidably causes the rearrangement of fine precipitations.

3. Trapped flux and stability

Zhou *et al.* [13] successfully solved the liquid source leakage problem, even at a T_{\max} of 1100°C, as a result of making the seeded infiltration and growth of the Gd123 single grain using a YBa₂Cu₃O_y pressed pellet as the liquid source supply. To develop this process, a simple but essential modification to insert a liquid source pellet at the bottom of the pre-form was made in the top-seed melt growth process. The trapped flux density of the sample without a liquid source substrate increases with the reduced thickness and reaches a peak value of 0.26 T after 2 mm of its thickness has been ground away, and then it decreases monotonously. The trapped flux density of 0.17 T was measured in the sample with a Y123 pellet substrate only 1.5 mm thick, indicating full growth until the very bottom. This is a very effective way to improve the trapped flux ability.

Concerning the trapped flux stability, Fig. 2 exhibits the trapped flux measured at different positions along the normal direction, from the centre of the surface of the Gd123 bulk with 0.4 mol% Fe-B addition. The sample was magnetized with field cooling down to 30 K under a stationary applied field of 5 T. The trapped field was successfully stabilized as a function of time. The results clearly show that the trapped flux would become stable after removing the external static field within 55 min. The results show a specific flux distribution along the c -axis and its stability.

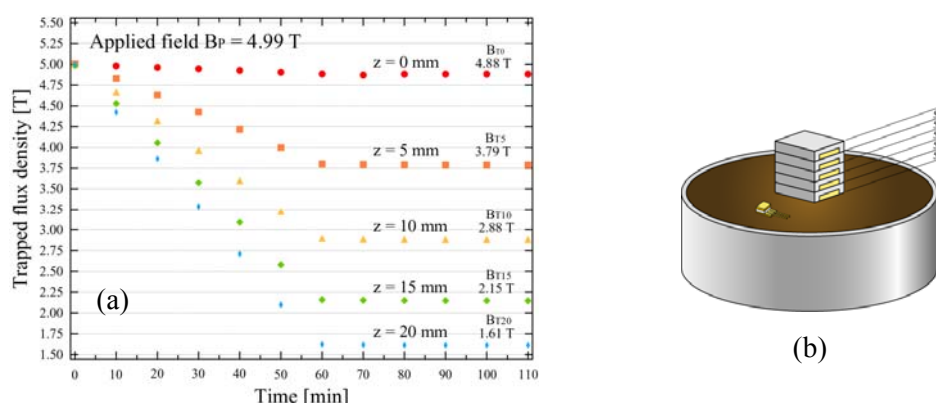


Fig. 2 Trapped magnetic flux density measured by stacked Hall sensors at different positions along the normal to the surface for Gd123 with 0.4 mol% Fe-B addition. The trapped field is successfully stabilized as a function of time at 30 K.

4. Conclusion

By exploring the processing procedure, heat treatment profile, seeding technology, and annealing conditions, the optimal growth conditions for processing high-textured RE-Ba-Cu-O single grains/domains have been achieved. The cold seeding melt-growth technology employing Nd-Ba-Cu-O/MgO thin films as seed crystals allows the batch processing of high performance Gd-Ba-Cu-O bulks. Furthermore, it was found that supplying greater sufficient liquid source during the melt growth benefits the homogenous distribution of $\text{Gd}_2\text{BaCuO}_5$ in a large-scale matrix, leading to a significant enhancement of the trapped magnetic field.

Acknowledgments

This work was partly performed using facilities of the ISSP, the University of Tokyo. The authors are grateful to the National Natural Science Foundation of China (NSFC, Grant No.11004129).

References

- [1] Tomita M and Murakami M 2003 *Nature* **421** 517.
- [2] Nariki S, Sakai N and Marakami M 2005 *Supercond Sci Technol* **18** 126.
- [3] Xu K, Zhou D, Li B, Hara S, Tsuzuki K, Zhang Y, Xu Y and Izumi M 2012 *Superconductivity: Recent Developments and New Production Technologies* Chapter 5 ed. Mularidhar Miryara (Nova Science Pub Inc).
- [4] Ishii Y, Shimoyama J, Tazaki Y, Nakashima T, Horii S and Kishio K 2006 *Appl. Phys. Lett.* **89** 202514.
- [5] *Handbook of High Temperature Superconductivity: Theory and Experiment* 2007 eds. Schrieffer J R and Brooks J S (Springer).
- [6] Xu CX, Hu A, Sakai N, Izumi M and Hirabayashi I 2005 *Supercond. Sci. Technol.* **18** 229.
- [7] Hu A, Xu CX, Izumi M, Hrabayashi I and Ichihara M 2006 *Appl. Phys. Lett.* **89** 192508.
- [8] Xu Y, Izumi M, Tsuzuki K, Zhang Y, Xu CX, Murakami M, Sakai N and Hirabayashi I 2009 *Supercond. Sci. Technol.* **22** 095009.
- [9] Xu K, Tsuzuki K, Hara S, Zhou D, Zhang Y, Murakami M, Nishio-Hamane D and Izumi M 2011 *Supercond. Sci. Technol.* **24** 085001.
- [10] Tsuzuki K, Hara S, Xu Y, Morita M, Teshim H, Yanagisawa O, Noudem J, Harnois Ch and Izumi M 2011 *IEEE Trans. Appl. Supercond.* **21** 2714.
- [11] Li B, Zhou D, Hara S, Xu K and Izumi M 2013 *IEEE Trans. Appl. Supercond.* **23** 8001804.
- [12] Li B, Zhou D, Xu K, Tsuzuki K, Zhang JC and Izumi M 2013 *Physica C* <http://dx.doi.org/10.1016/j.physc.2013.06.017>
- [13] Zhou D, Hara S, Li B, Xu K, Noudem J and Izumi M 2013 *Supercond. Sci. Technol.* **26** 015003